V European Conference on Computational Fluid Dynamics
ECCOMAS CFD 2010
J. C. F. Pereira and A. Sequeira (Eds)
Lisbon, Portugal,14-17 June 2010

ROBUST OPTIMIZATION OF DENSE GAS FLOWS UNDER UNCERTAIN OPERATING CONDITIONS

P. Cinnella*, S.J. Hercus*

*Laboratoire DynFluid
Arts et Métiers ParisTech
151 Bd de l'Hôpital, 75013 Paris, France
e-mail: paola.cinnella@paris.ensam.fr

Key words: Uncertainty Quantification, Polynomial Chaos, Robust Optimization, Dense Gas Dynamics

Abstract. *A robust optimization procedure based on a multi-objective genetic algorithm (MOGA) is used to generate airfoil profiles for transonic inviscid flows of dense gases, subject to uncertainties in the upstream thermodynamic conditions. The effect of the random variations on system response is evaluated using a non-intrusive Polynomial Chaos (PC) based method known as the Probabilistic Collocation Method (PCM). After initial PCM simulations which showed that the dense gas system was highly sensitive to input parameter variation, a multi-objective genetic algorithm coupled to the PCM produced a Pareto front of optimized individual geometries which exhibited improvements in mean performance and/or stability over the baseline NACA0012 airfoil. This type of analysis is essential in improving the feasibility of Organic Rankine Cycle (ORC) turbines, which are typically designed to recover energy from variable sources such as waste heat from industrial processes.*

1 INTRODUCTION

Dense gases are defined as single phase vapors, characterized by complex molecules and moderate to large molecular weights. Flows of dense gases are of considerable interest for many applications in energy production,[1–3] refrigeration,[4,5] and chemical processing.[6] For dense gases operating at temperatures and pressures of the same order of magnitude of their critical point, the ideal gas approximation is no longer valid and real gas effects become influential in the dynamic behavior of the fluid. Real gas effects are particularly strong for highly complex molecules which display a non-monotonic variation of the sound speed with respect to pressure. Some fluids characterized by particularly high molecular complexity have been theoretically predicted[7–10] to display a region of negative values of the Fundamental Derivative of Fluid Dynamics[11] Γ in the vapor phase. This thermodynamic region is called the inversion zone[12] and the locus of thermodynamic states in the vapor phase such that $\Gamma < 0$ is referred to as the transition line. Fluids of this type are said to possess Bethe-Zel'dovich-Thompson (BZT) properties. For transonic flows of BZT type fluids, compression shock waves may be suppressed if the upstream thermodynamic conditions are selected within the inversion zone, since for $\Gamma < 0$ compression shocks violate the second principle of thermodynamics.[12] Harnessing the unusual properties of BZT type fluids could potentially have a significant impact on the performance of low temperature energy conversion cycles, such as in the case of Organic Rankine Cycle (ORC) turbines.[2,3,13]

Whereas a traditional Rankine Cycle operates with water vapor as the working fluid, ORC turbines use an organic fluid such as hydrocarbons, silicon oils or other organic refrigerants. The low critical temperature, high density and elevated heat capacities of these fluids result in high suitability for low temperature operation, even as low as 80°C.[14] Furthermore, the slope of the saturated vapor line for organic fluids eliminates the risk of condensate at the turbine outlet, without heating the working fluid into the superheated vapor region. ORCs represent a promising technology for the development of widely distributed, small yield (less than 1MW) thermal energy conversion devices.[15] Additional practical advantages are the self lubricating nature of organic fluids and the absence of a superheating requirement. ORC turbines typically utilize a single-stage turbine operating in the transonic/supersonic regime, where a major source of losses arises from the formation of shock waves and their interaction with boundary layers. The use of organic fluids possessing BZT properties could potentially avoid shock formation and the consequent losses, if only turbine expansion occurred entirely within or very close to the inversion zone.

In order to improve the feasibility of BZT flows in ORC turbines, a compromise is suggested by Cinnella & Congedo.[16] The proposition is to allow the dense gas flow to evolve partially outside the inversion zone, thus permitting loss inducing compression shocks and mixed waves. Such waves are expected to be relatively weak if the thermodynamic states on either side of the discontinuity are in the vicinity of the transition line.[12] These weak

waves would result in associated losses which are lower than in the case of an ideal gas, leading to increased turbine efficiency. Operating the turbine cascade partially outside the inversion zone also allows for a larger difference between the maximum and minimum temperature of the thermodynamic cycle, boosting the overall power output. However, this approach of allowing variation in the upstream thermodynamic state of the dense gas flow introduces a complex challenge at the modeling stage of development.

ORC turbines are often designed to exploit waste heat from other processes, where inlet operating conditions are likely to be highly variable. For the BZT working fluids currently considered, the inversion zone, where the turbine isentropic efficiency is expected to be the most favorable, is found to be relatively small and in close proximity to the saturated vapor curve. As a result, variations in upstream thermodynamic conditions may induce dramatic changes in the flow physics and ultimately in the system performance. Given the relatively small size of the inversion zone and the variability of proposed energy sources, the physical behavior of the system is likely to be highly sensitive and difficult to model using a classic approach. The variability of the operating conditions represents a crucial issue for all ORC turbines, not restricted to those using BZT working fluids. Another important point is that the serialization of ORC turbogenerators leads to the development of a standard turbine geometry which is applied to a relatively wide range of situations. As a consequence, even when turbine admission conditions remain relatively stable for a given application, the final performance may vary considerably according to the proximity of these conditions to the design point. Taking account of the variability of operating conditions is therefore critical to ensure optimal turbine performance and durability. This variability can be evaluated implementing a non-deterministic (i.e. stochastic) approach known as uncertainty quantification. This type of analysis consists of measuring the system response to random and unknown variations in input parameters. Dense gas flows are particularly suited to stochastic analysis due to their high sensitivity to variations in upstream thermodynamic conditions. A recent study[17] has already applied a stochastic analysis to a BZT type dense gas flow simulation over an airfoil in order to quantify the effect of uncertainties of parameters in different models of the Equation of State (EOS).

The most basic type of stochastic analysis is the Monte Carlo (MC) method, which consists of randomly sampling N values of an input variable with a known or supposed input distribution, and then calculating the deterministic solution for each input value. Theoretically, the MC method will converge to the exact stochastic solution when the number of samples $N \to \infty$. In practice, several thousand samples are required to obtain an acceptable level of accuracy. As a result, the MC method is very computationally intensive when applied to fluid flow simulations. A more sophisticated class of stochastic analysis methods are known as the Polynomial Chaos (PC) methods. Essentially a spectral approach, PC methods can provide detailed statistical information of system response to input parameter variations at a fraction of the computational cost of the MC method. PC methods can efficiently obtain accurate estimates of uncertainty for models which describe physical phenomena in terms of partial differential equations, even in situations

exhibiting strong non-linear dependence on random input variations.[18] The classic PC approach is an intrusive method, which requires significant modifications of the underlying CFD flow solver. However, a non-intrusive method is preferable to increase the flexibility of the stochastic analysis for complex CFD problems, as the simulation is considered an independent "black box"and direct modification of the CFD code is not required Several PC based non-intrusive methods have been proposed in the literature[19–21] In the present study, the Probabilistic Collocation Method (PCM) proposed by Loeven et al.[19,20] is selected due to its exponential convergence and non-intrusive properties.

The aim of the present work is to demonstrate the feasibility and usefulness of robust design techniques for dense gas flows, given uncertainties applied to the upstream thermodynamic conditions. The robust design procedure involves the use of a PCM stochastic solver coupled with a multi-objective genetic algorithm (MOGA). At this early stage of the research work, we focus our attention on a simplified geometry, namely an airfoil placed into a dense gas stream with randomly varying thermodynamic conditions. The study is divided into two main sections. The first section considers uncertainty quantification applied to transonic dense gas flows using a Polynomial Chaos (PC) based stochastic approach known as the Probabilistic Collocation Method (PCM). The PCM algorithm, initially validated for complex flow problems in Hercus,[22] is then applied to an existing solver[23] of a inviscid transonic dense gas flow over half of a symmetrical NACA0012 airfoil at $M_\infty = 0.95$. The working fluid used is *pf-perhydrofluorene* ($C_{13}F_{22}$, commercially known as PP10) with the thermodynamic properties modeled by the Martin-Hou equation of state. The aerodynamic performance of the airfoil at 0° incidence is examined with Gaussian random variations in the upstream pressure and temperature.

In the second section of this study, a PCM stochastic analysis is coupled with an existing multi-objective Pareto-based genetic algorithm (MOGA), previously applied to transonic dense gas flows.[24–26] The robust optimization procedure generates a series of optimized 2D airfoils for dense gas flows, based on minimization of the mean and standard deviation of the drag coefficient. The high computational cost of the genetic algorithm is mitigated by the use of the Richardson extrapolation method (REX) on each individual calculated. This mesh extrapolation method, already applied to robust profile optimization of dense gas flows,[26] accelerates convergence and increases the solution accuracy for each individual, which can improve MOGA convergence. Optimal individual geometries from the MOGA optimization process are selected and their aerodynamic performance analyzed and verified with both deterministic and stochastic simulations. Finally, a posteriori testing of the optimized individuals is carried out in the turbulent flow regime using the Baldwin-Lomax turbulence model.

2 GOVERNING EQUATIONS AND FLOW SOLVER

2.1 Physics of dense gas flows

In this study, we focus our attention on a class of dense gases of the retrograde type (gases which superheat when expanded) known as Bethe-Zel'dovich-Thompson (BZT) fluids. In a specific range of thermodynamic conditions in the vapor region, BZT gases exhibit non-classical dynamic behavior, such as expansion shock waves, mixed shock/fan waves and splitting shocks. This unusual behavior arises when the value of the *Fundamental Derivative of Gas Dynamics*[11] $\Gamma = 1 + \frac{\rho}{a}\left(\frac{\partial a}{\partial \rho}\right)_s$, becomes negative. Note that a represents the speed of sound, ρ the fluid density and s the entropy of the fluid. The fundamental derivative measures the rate of change of the sound speed in isentropic perturbations. For perfect gases, $\Gamma = (\gamma + 1)/2 > 1$, where γ (the specific heat ratio of the fluid) is strictly greater than 1 due to thermodynamic stability requirements. For the majority of classical working fluids, an isentropic compression leads to an increase in the speed of sound.

For a BZT fluid, if $\Gamma < 1$, then $(\frac{\partial a}{\partial \rho}) > 1$, and the flow exhibits a reversed variation in the speed of sound, where a grows in isentropic expansions and falls in isentropic compressions. An important consequence of this phenomenon is observed when considering a weak shock wave. It can be shown (Cramer & Kluwick[12]) that the entropy difference Δs across the shock is given by the expression:

$$\Delta s = \frac{-a^2 \Gamma}{v^3} \frac{(\Delta v)^3}{6T} + O\left((\Delta v)^4\right) \tag{1}$$

where Δ is the change in a fluid property across the shock, $v = 1/\rho$ is the specific volume, and T is the absolute temperature. It follows that in regions where $\Gamma < 0$, compression shocks cannot form as a consequence of the entropy inequality, whereas expansion shocks are theoretically admissible. The region where $\Gamma < 0$ is referred to as the *inversion zone*, and the $\Gamma = 0$ contour is known as the *transition line*. These features can be observed on the state diagrams shown in Figure 1 for the heavy perfluorocarbon *pf-perhydrofluorene*, commercially known as PP10. The thermodynamic properties of this gas are modeled using the realistic Martin-Hou equation of state. The T-s diagram displayed in Figure 1 shows the retrograde behavior of the fluid: the liquid/vapor coexistence curve exhibits a positive slope up to near-critical conditions.

Numerical simulation of BZT flows over isolated airfoils and wings[27,28] has shown that with a negative upstream value of Γ, the flow remains subsonic throughout the entire domain, whereas a shock is observed for a perfect gas at the same operating conditions. BZT effects can essentially delay shock wave formation and the related losses, increasing the critical Mach number to near-sonic speeds. This is in clear contrast to the classical behavior of regular gases such as air, oxygen, nitrogen and steam that exhibit much lower critical Mach numbers (around 0.8 or even less). As a result of further numerical simulations conducted by Brown & Argrow,[2] Cinnella et al.[29] and Congedo et al.,[30] the

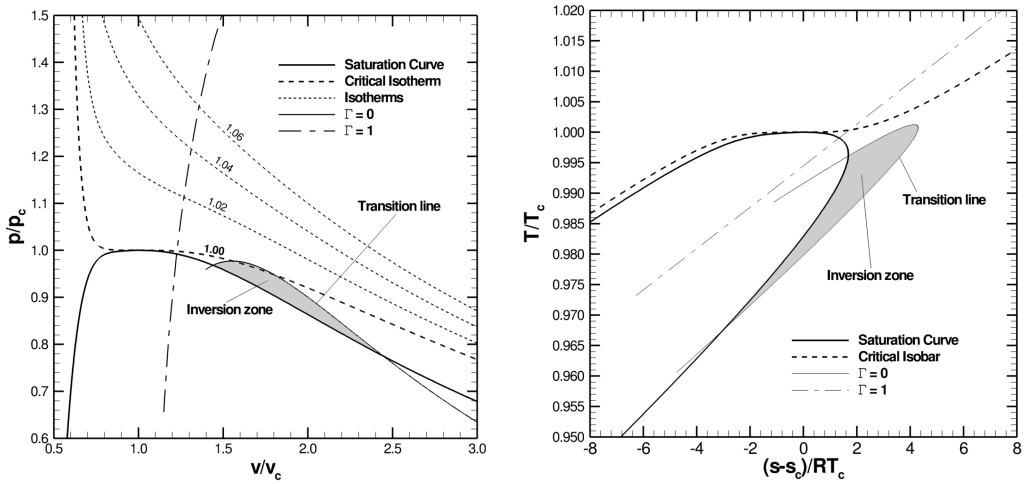

Figure 1: (left) Pressure-volume diagram and (right) temperature-entropy diagram for PP10 ($C_{13}F_{22}$) using the Martin-Hou equation of state. The subscript c represents a critical value.

conclusion has been made that the use of BZT fluids in turbine design could lead to a potential increase in efficiency of approximately 3-8%, with advancement in fluid dynamic design and non-classical effect exploitation.

2.2 Dense gas model and flow solver

Dense gas flows are governed by the equations for equilibrium for non-reacting flows. In the present study we consider the Euler equations, written in integral form for a control volume Ω with boundary $\partial\Omega$:

$$\frac{d}{dt}\int_{\Omega} \boldsymbol{w}\, d\Omega + \int_{\partial\Omega} \boldsymbol{f}\cdot\boldsymbol{n}\, dS = 0 \tag{2}$$

In equation (2), $\boldsymbol{w}$ is the conservative variable vector, $\boldsymbol{n}$ is the outer normal to $\partial\Omega$, and $\boldsymbol{f}$, is the flux density:

$$\boldsymbol{w} = (\rho, \rho\boldsymbol{v}, \rho E)^T \quad ; \quad \boldsymbol{f} = \left(\rho\boldsymbol{v}, \rho\overline{\overline{I}}, \rho\boldsymbol{v}\boldsymbol{v}, \rho\boldsymbol{v}H\right)^T$$

where $\boldsymbol{v}$ is the velocity vector, E the specific total energy, $H = E + p/\rho$ the specific total enthalpy, p is the pressure and is the unit tensor. The preceding equations are completed by a thermal equation of state, $p = p\left(\rho(\boldsymbol{w}), T(\boldsymbol{w})\right)$, and by a caloric equation of state for the specific internal energy e, which must satisfy the compatibility relation:

$$e = e\left(\rho(\boldsymbol{w}), T(\boldsymbol{w})\right) = e_r + \int_{T_r}^{T} c_{v,\infty}(T')\, dT' - \int_{\rho_r}^{\rho}\left[T\left(\frac{\partial p}{\partial T}\right)_{\rho} - p\right]\frac{d\rho'}{\rho'^2} \tag{3}$$

In Equation (3), $c_{v,\infty}$ is the ideal gas specific heat at constant volume, quantities with a prime superscript are auxiliary integration variables, and subscript r indicates a reference state. In the present work, the gas response is modeled through the comprehensive

thermal equation of state of Martin & Hou,[31] which provides a realistic description of the gas behavior close to saturation conditions[32,33] and requires just a minimum amount of thermodynamic input data. Further detail concerning the Martin-Hou model and the variation law for $c_{v,\infty}$ is presented in Cinnella & Congedo.[25] The governing equations are discretized using a cell-centered finite volume scheme for structured multi-block meshes of third-order accuracy, which allows the computation of flows governed by an arbitrary equation of state. A study of the accuracy of the numerical solver has been demonstrated in previous works,[16,23] and is not discussed further.

3 UNCERTAINTY QUANTIFICATION FOR DENSE GAS FLOWS

3.1 Polynomial chaos methods for uncertainty quantification

Recent research by Loeven et al.,[19,20] has developed an efficient non-intrusive variation on the standard Generalized Polynomial Chaos (GPC) method. Based on the idea of a standard chaos transformation, the Probabilistic Collocation Method (PCM) approach consists of two important modifications to the classic method. Firstly, a chaos version of Lagrange interpolation is used to approximate the chaos polynomial, even with a minimum of two collocation points. The second modification is to use Gaussian quadrature to compute the Galerkin projection and the integration of the distribution function approximation. In terms of calculation cost, both PC methods show significant improvements over the MC analysis, and demonstrate exponential convergence with respect to the order of the polynomial. For increasing values of the polynomial order, the PCM requires more deterministic calculations than in the GPC case. Although this would suggest that the GPC method is more rapid, the non-intrusive nature of the PCM provides a substantial increase in flexibility. The PCM is therefore particularly suited to the study of complex CFD simulations, without requiring modification to the CFD code framework. The PCM is therefore the stochastic method used in the present study.

In practical terms, the Probabilistic Collocation method consists of calculating the deterministic solution at selected points (nodes) in the input distribution, then multiplying the solutions by a weighting function in order to compute output statistical information. As in the GPC method, each input distribution is associated with a corresponding orthogonal polynomial according to the Askey scheme (summarized in Xiu & Karniadakis[34]). For example, in the case of a normal or Gaussian input distribution, the corresponding quadrature polynomial is the Hermite polynomial. Here the PCM is presented considering the case of a Gaussian random input distribution, thus Gauss-Hermite chaos quadrature is employed to compute the Galerkin projection. For the case of a velocity field u subjected to random input variable fluctuations $\xi(\theta)$, the solution is decomposed into deterministic: $u_i(\boldsymbol{x},t)$, and stochastic: $h_i(\xi(\theta))$, parts:

$$u\left(\boldsymbol{x},t,\xi(\theta)\right) = \sum_{i=1}^{P_{PCM}} u_i(\boldsymbol{x},t)\, h_i(\xi(\theta)) \quad \text{where} \quad h_i(\xi(\theta)) = \prod_{\substack{k=1 \\ k\neq i}}^{N_p} \frac{\xi(\theta)-\xi(\theta_k)}{\xi(\theta_i)-\xi(\theta_k)} \tag{4}$$

where $u_i(\boldsymbol{x}, t)$ is the is the deterministic solution at the collocation point θ_i. In the PCM, p is the order of the quadrature polynomial and the number of collocation points is given by $P_{PCM} = p^n$, where n represents the number of random input variables. The term h_i is the Lagrange interpolating polynomial chaos of order $N_p = p - 1$ that passes through the P_{PCM} collocation points, with $h_i\left(\xi(\theta_k)\right) = \delta_{ik}$. The collocation points θ_i are chosen such that they correspond to the Gaussian quadrature points, which are simply the roots of the quadrature polynomial. Finally, in order to compute the statistics of the output, the solution is integrated using Gauss-Hermite chaos quadrature where the quadrature nodes correspond to the collocation points θ_i. The output mean μ_u and variance σ_u^2 are determined by:

$$\mu_u = \sum_{i=1}^{P_{PCM}} u_i(\boldsymbol{x}, t)\, w_i \quad ; \quad \sigma_u^2 = \sum_{i=1}^{P_{PCM}} \left(u_i(\boldsymbol{x}, t)\right)^2 w_i - (\mu_u)^2 \tag{5}$$

where the w_i values correspond to the Gauss-Hermite weights. In the case of multiple input variables, the PCM is slightly modified. The transformed input vector becomes $\boldsymbol{\xi}(\theta) = \{\xi_{s=1}(\theta), \xi_{s=2}(\theta), \cdots, \xi_{s=n}(\theta)\}$, and the stochastic part of Equation (4) can be rewritten in vector form:

$$h_i(\xi(\theta)) = \prod_{s=1}^{n} \left[\prod_{\substack{k=1 \\ k \neq i}}^{N_p} \frac{\xi(\theta) - \xi(\theta_k)}{\xi(\theta_i) - \xi(\theta_k)} \right] \tag{6}$$

In order to determine output statistics given multiple uncertain input parameters, Equation (5) must be analytically determined with the multivariable PC expansion (c.f. Equation (9), Xiu & Karniadakis[34]) and the standard definitions of the statistical moments. This procedure is relatively time consuming and complex, especially with several uncertain input variables (i.e. high values of s). A more practical approach to determine the solution statistics is to reconstruct the problem using a simple MC method on the Lagrange interpolation equation, denoted the Reconstructed Monte Carlo method (RMC). Once the deterministic solution at each collocation point, $u_i(\boldsymbol{x}, t)$, has been determined, a MC analysis is used to generate a large number, M, of values for $\xi_s(\theta)$, thereby constructing M possible variations of $h_i(\xi(\theta))$. Since Equation (4) is linear in the terms $u_i(\boldsymbol{x}, t)$, the RMC can be carried out inexpensively for large values of M. The result is a complete set of output solutions, from which the statistical moments can be easily calculated. The PCM analysis coupled with the RMC has been validated for complex flow problems in Hercus,[22] and for brevity is not presented in this work.

3.2 Stochastic analysis of a transonic dense gas flow over the NACA0012 airfoil

The non-intrusive Probabilistic Collocation Method (PCM) stochastic analysis was coupled to an existing dense gas code developed by Cinnella & Congedo[23] to model the

flow of a BZT type retrograde dense gas fluid over one half of a symmetrical NACA0012 airfoil at 0° incidence. The upstream Mach number was set to $M_\infty = 0.95$. The upstream thermodynamic conditions were fixed in terms of critical point values at $p/p_c = 0.91$ and $T/T_c = 1.02$. In these conditions $\Gamma = 0.43$, which represents an operating point just outside the inversion zone. For this choice of the operating conditions, the flow over the airfoil is transonic and shock waves are formed at both airfoil surfaces. Due to the symmetrical nature of the flow, only half of the domain is simulated by explicitly enforcing a symmetry condition. A slip boundary condition was imposed on the surface of the airfoil and non-reflecting boundary conditions are used at the far-field boundaries. Three structured half-C grids were created to discretize the fluid domain, and the far-field boundary was located approximately 10 chords away from the airfoil. The grid convergence was studied by observing the drag coefficient C_D obtained from the three different grids for an initial set of deterministic simulations. The C_D results are shown in Table 1, where the calculation times are obtained with an Intel© Xeon© W3503 CPU with a 2.40 GHz clock speed. To reduce the computational cost with respect to fine-grid computations while preserving a comparable accuracy on the computed aerodynamic coefficients, the Richardson Extrapolation (REX) method was applied to results from the coarse and medium grids. The details of this method are presented in Cinnella & Congedo[26] and will not be outlined here. The advantage of the REX method was a reduced calculation time with the same level of accuracy as the fine grid solution. For this reason, the following computations are carried out using the REX method applied, using the coarse and medium grids.

Grid	**Number of cells**	C_D	**Iterations**	**Residual** (10^x)	**Calculation Time** (MM:SS)
Coarse	50×16	0.0728	5000	-6.0	01:22
Medium	100×32	0.0724	7000	-9.0	08:18
Fine	200×64	0.0723	10000	-5.6	46:25
Richardson Extrapolation (REX)	*Coarse + Medium*	0.0723	*4000 + 5000*	-10.2	07:11

Table 1: Drag coefficient C_D results for the deterministic dense gas simulations.

A stochastic analysis was carried out in order to examine operating point variability on the dense gas flow simulation. The non intrusive PCM approach was used to study the effects of Gaussian random variations about the upstream states of $p/p_c = 0.91$ and $T/T_c = 1.02$, with the input coefficients of variation CV set to 1.0% and 2.3% respectively. The Hermite polynomial was used, and a Reconstructed Monte Carlo (RMC) method with $M = 10000$ linear simulations was used on the Lagrange interpolating polynomial in order to generate a complete set of output solutions. The PCM analysis was implemented with chaos polynomials of order $N_p = 2$ and $N_p = 3$ to enable a study of the stochastic method convergence properties. The location of the thermodynamic operating conditions of the collocation points can be observed on the $p - v$ diagram in Figure 2.

Results for the mean μ, standard deviation σ, and the coefficient of variation CV of the

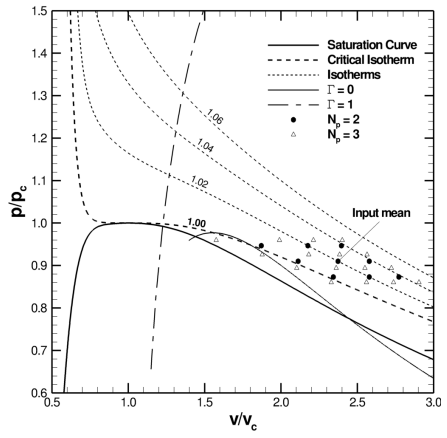

Figure 2: Input collocation points for the stochastic PCM analysis.

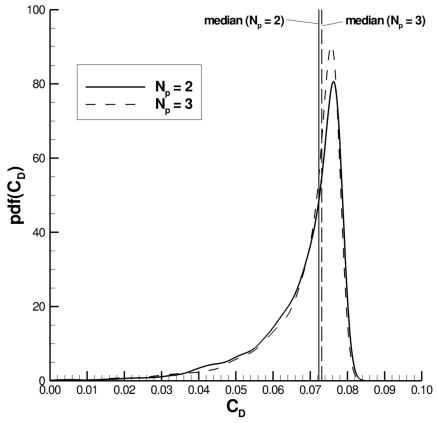

Figure 3: Probability density function of the drag coefficient C_D (REX method).

drag coefficient C_D obtained by the PCM for $N_p = 2$ and $N_p = 3$ are shown in Table 2. Good agreement is observed between the results of increasing polynomial order. In both cases the stochastic solution exhibits a high sensitivity to input parameter variation, due to the relatively significant changes in physical flow behavior. Several collocation points lie within or very close to the inversion zone, resulting in a reduction in C_D due to the reduced magnitude of the compression shocks. As a result, the mean drag coefficient obtained by the stochastic simulation is lower than in the case of the deterministic simulation at the input mean (DSIM). Using the complete set of output solutions obtained by the RMC method on the PCM solutions, a probability density function of the C_D can be generated (Figure 3). The distribution of the output C_D is clearly non-Gaussian, due to the non-linearity of the dense gas system. In physical terms, Figure 3 shows that a random Gaussian variation in an operating point close to the saturation curve results in a non-Gaussian distribution of the drag coefficient which tends towards the low drag side. This is confirmed with a skewness value of -2.2.

N_p	Number of deterministic solutions	$\mu(C_D)$	$\sigma(C_D)$	$CV(C_D)$
2	9	0.0682	0.0120	17.5%
3	16	0.0685	0.0123	17.9%
DSIM	1	*0.0723*	-	-

Table 2: Results of the drag coefficient C_D (REX method), for the PCM stochastic analysis.

Further evidence of the high sensitivity of the dense gas simulation to operating point variability is visible by the large size of the error bars in Figure 4. The largest contributor of variability the position and magnitude of the oblique shock, which is directly affected by the reduction of the fundamental derivative Γ for operating points close to the inversion zone. Figure 4 confirms the base of the shock as a principal source of solution variation, with the largest values in standard deviation of the Mach number observed in this region. The uneven representation of the shock waves in Figure 4 occurs due

to the limited number of deterministic solutions used to model the discontinuity. These discrete individual deterministic solutions at the collocation points can be seen in Figure 5 for the pressure coefficient C_p over the NACA0012 profile for the PCM analysis with $N_p = 3$ (therefore $P_{PCM} = 16$). This figure clearly shows that compression shocks can be avoided if the upstream operating point is located within the inversion zone. Using the complete set of output solutions generated by the RMC method, it is possible to determine the percentiles of the output solution (Figure 5) and provide an envelope of possible C_p values. Note that the median and the mean solutions are not coincident, suggesting the presence of non-Gaussian effects. Figure 6 confirms this non-Gaussian behavior with probability density functions of the pressure coefficient at two points on the surface of the airfoil. Good overall convergence of the stochastic method is observed in Figure 6 with the close accordance of the local solution distributions obtained by the $N_p = 2$ and $N_p = 3$ simulations. However, the increased solution variability close to the shock region ($x/c = 0.9$) slightly reduces the quality of this convergence. In the following section of this work where a robust optimization of the airfoil profile is carried out, a polynomial chaos order of $N_p = 2$ is selected in order to reduce scalar computation time. In the near future, efficient parallelization of the robust optimization procedure will permit the use of higher order polynomial chaos. Despite the limited number of deterministic solutions used compared with the classic MC method, the stochastic PCM analysis coupled with the RMC method can be used to provide critical uncertainty information for use in an engineering application with a reduced computational effort.

4 ROBUST OPTIMIZATION UNDER UNCERTAIN OPERATING CONDITIONS

4.1 Robust optimization with a Multi-Objective Genetic Algorithm (MOGA)

In spite of their relatively high computational cost, genetic algorithms have been successfully applied to aerodynamic shape optimization to a transonic dense flows.[24–26] Evolutionary optimization strategies employed in Pareto based genetic algorithms are a flexible and robust means of determining global optima of multi-point problems. Implementation is relatively straightforward without significant code modification, as only the evaluation of selected objective functions for each individual is required. In this study, the PCM stochastic analysis of transonic dense gas flows presented earlier is coupled to an existing multi-objective genetic algorithm (MOGA), based on the Non-Dominated Sorting Algorithm proposed by Srinivas and Deb.[35,36]

In this study, the MOGA was used to generate a series of optimized symmetrical 2D airfoils for dense gas flows, based on minimization of the mean and standard deviation of the drag coefficient. 28 generations of 36 geometries were obtained, resulting in over 800 stochastic PCM analyses carried out (duplicated geometries were not recalculated). Each individual PCM analysis was calculated with a chaos polynomial of order $N_p = 2$ (requiring 9 deterministic simulations), which resulted in an overall calculation time of

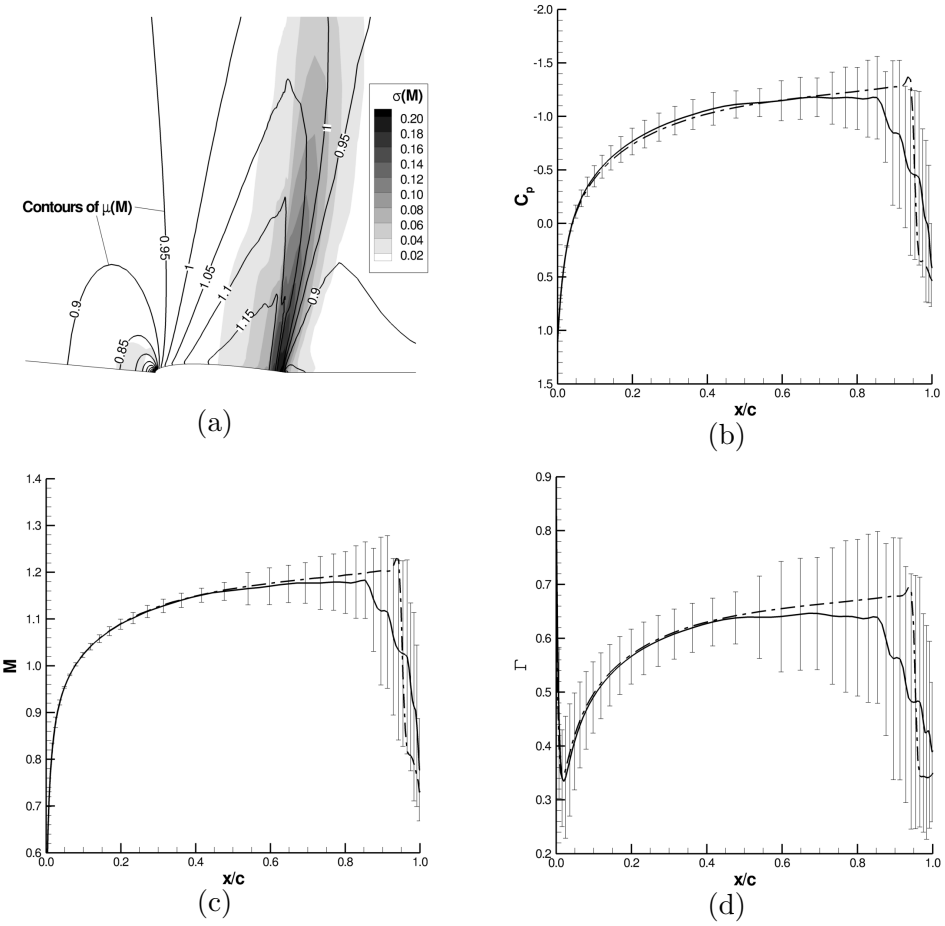

Figure 4: Stochastic PCM results on the medium grid (100×32) with $N_p = 3$. (a) Contours of $\mu(M)$ and $\sigma(M)$. (b) C_p, (c) M (d) Γ over the airfoil $x/c \in [0, 1]$. Solid lines represent the mean solution, dotted lines represent the DSIM solution. The error bars represent $\pm\sigma$.

over 40 days on an Intel© Xeon© W3503 2.4 GHz processor. The high computational cost of the genetic algorithm was mitigated by the use of the Richardson extrapolation method (REX) on each individual calculated. This solution extrapolation method, already applied to robust profile optimization of dense gas flows,[26] accelerates convergence and increases the solution accuracy for each individual. Furthermore, Cinnella & Congedo[26] show that an increase in solution accuracy can improve MOGA convergence. The structure of the code for the robust optimization algorithm coupled with the stochastic dense gas analysis is strongly modular and is therefore very well suited for parallel operation. This is a critical point when considering potential industrial applications such as the design of ORC turbines, where more complex and costly CFD simulations would be required. A complete parallelization of the MOGA and of the PCM solver are warranted as forthcoming work. For comparison, a deterministic single parameter optimization was also carried out for 28 generations of 36 individuals, with only the drag coefficient as the minimization function.

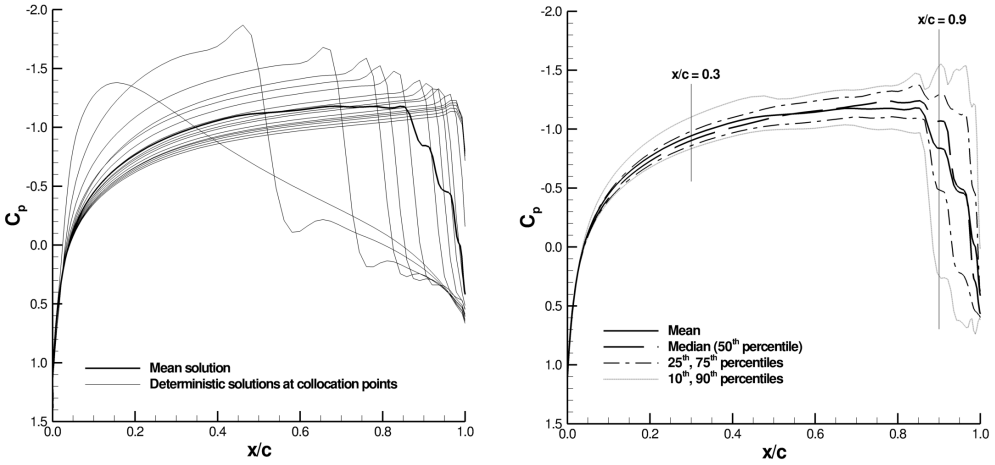

Figure 5: (left) Pressure coefficient C_p over the NACA0012 profile for each deterministic solution at the 16 collocation points with $N_p = 3$ and (right) percentiles of the pressure coefficient over the profile.

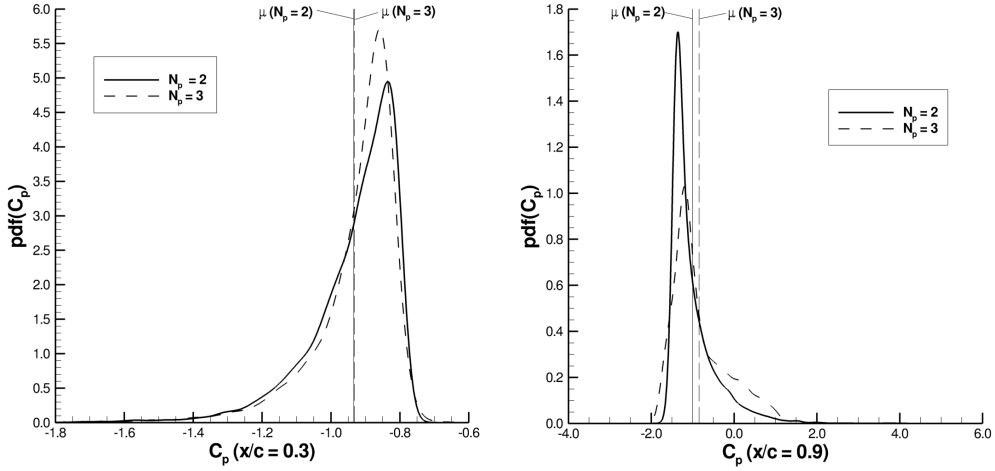

Figure 6: Probability distribution functions for the pressure coefficient C_p at two points on the airfoil surface, for the $N_p = 2$ and $N_p = 3$ cases. The mean C_p values are shown by the vertical lines.

With only a single deterministic simulation to be carried out for each individual at $p/p_c = 0.91$ and $T/T_c = 1.02$, the overall scalar calculation time was reduced by a factor of 9, however this left the variation of the solution uncontrolled. Finally, several optimized profiles were selected from both the deterministic and stochastic optimization procedures and their performance verified on the medium grid (100×32 cells) with a higher polynomial chaos order ($N_p = 3$). Since optimization based on an inviscid flow model may lead to airfoil shapes with low wave drag but with poor viscous behavior,[25] the airfoil performance was verified by applying the dense gas solver to the solution of the Reynolds-Averaged Navier-Stokes (RANS) equations completed by the algebraic Baldwin-Lomax turbulence model. We refer to Cinnella & Congedo[23] for details about the viscous flow solver. The

turbulent regime simulations were performed on a 160×64 half C-grid with a refined boundary layer.

4.2 Results of the robust optimization procedure

The mean and standard deviation of the drag coefficients C_D of all the solutions obtained from the stochastic robust optimization procedure are shown in Figure 7, including the final Pareto front and the stochastic results for the NACA0012 airfoil and the single parameter optimization (#753d). Several individuals in the Pareto front exhibited improvements in the $\mu(C_D)$ and $\sigma(C_D)$ over the standard NACA0012 airfoil. Very good agreement was observed between the Pareto front after 23 generations and the final 28 generations, indicating that convergence of the MOGA procedure was achieved. The final Pareto front was found to be non-convex, due to the non-linearity of the dense gas system. Three individual geometries were selected from the front to be examined in further detail (Figure 7): individual #258 with the lowest value of $\mu(C_D)$; individual #767 with a similar $\mu(C_D)$ to the NACA0012 but with an improved stability; and individual #791 as the most stable individual, with the lowest $\sigma(C_D)$. Note that for some industrial applications, a certain loss in mean performance may be acceptable if a highly stable solution is obtained. Finally, using a single objective deterministic optimization based solely on a low deterministic C_D, the lowest drag individual #753d is selected. The optimized geometries and the NACA0012 airfoil are shown in Figure 8. In the case of the lowest drag airfoils (#258, #753d), the point of maximum thickness is located downstream ($x \approx 0.55$) of the NACA0012 maximum thickness point. The more stable airfoil profiles (#767, #791) have a maximum thickness in approximately the same region as the NACA0012 airfoil ($x \approx 0.30$) but exhibit a more shallow trailing edge gradient compared to the other profiles. The only source of drag in the non-viscous simulations is the trailing edge compression shock, so any modification of the location or magnitude of this shock affects the overall drag coefficient for the airfoil.

A verification of the stochastic performance for $N_p = 3$ of the dense gas flow over the optimized airfoils is shown in Figure 9. Evidence of the instability of individuals #258 and #753d is observed by the small region of elevated values of $\sigma(M)$ at the base of the shock region. The the steep trailing edge gradient of these individuals induces an oblique and unstable trailing edge shock. In comparison, the most stable airfoil (#791) exhibits smaller values of $\sigma(M)$ spread over a larger region at the base of the shock. The shallow trailing edge gradients of these more stable individuals (#767 and #791) promote the formation of stronger shock waves. Although this induces a larger drag coefficient, the stability of the shock is improved and the variation of the drag coefficient is reduced. Good convergence of the stochastic PCM analysis was observed in the comparison of the drag coefficient data for $N_p = 2$ and $N_p = 3$ (Table 3). The hierarchy of stability was preserved in the higher order case, with individuals #258 and #753d exhibiting the highest CV values. The stochastic convergence of $\mu(C_D)$ and $\sigma(C_D)$ shown in Table 3 validates the selection of $N_p = 2$ in the MOGA to reduce the overall scalar computational effort.

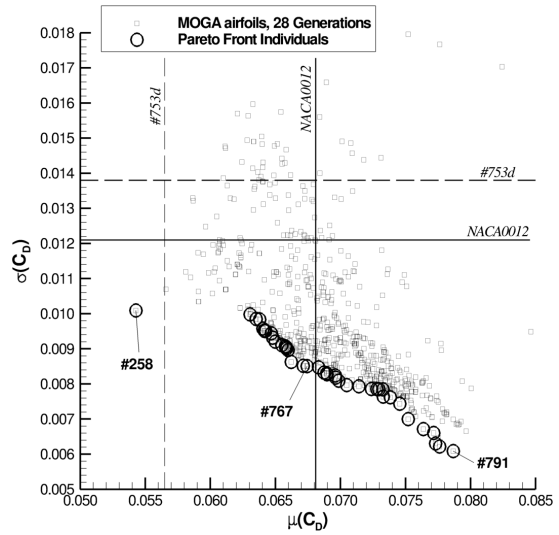

Figure 7: Final population generated by the two parameter PCM stochastic robust optimization problem. NACA0012 and the single parameter optimal individual (#753d) are also shown.

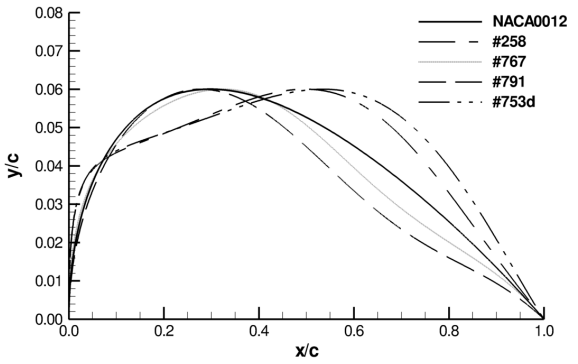

Figure 8: Geometries of selected optimized airfoils from the Pareto front. Also shown is the geometry obtained from the deterministic optimization (#753d) and the NACA0012 airfoil.

Airfoil		$N_p = 2$			$N_p = 3$		
Geometry	$\boldsymbol{C_D(DSIM)}$	$\boldsymbol{\mu(C_D)}$	$\boldsymbol{\sigma(C_D)}$	$\boldsymbol{CV(C_D)}$	$\boldsymbol{\mu(C_D)}$	$\boldsymbol{\sigma(C_D)}$	$\boldsymbol{CV(C_D)}$
NACA0012	0.0722	0.0682	0.0120	17.5%	0.0685	0.0123	17.9%
#258	0.0595	0.0573	0.0104	18.7%	0.0566	0.0116	20.5%
#767	0.0717	0.0687	0.0083	12.1%	0.0690	0.0095	13.8%
#791	0.0803	0.0782	0.0060	7.7%	0.0782	0.0079	10.1%
#753d	0.0599	0.0565	0.0138	24.5%	0.0567	0.0130	22.9%

Table 3: Drag coefficients (REX grid) for optimized airfoils, $N_p = 2$ and $N_p = 3$.

As a final validation of the performance of the optimized individuals, a series of simulations in the turbulent regime was carried out using the Baldwin-Lomax turbulence model on a 160×64 cell grid with a refined boundary layer. The performance of the optimized airfoils is summarized in Table 4, where the mean, standard deviation and DSIM drag coefficients are presented. The total viscous drag coefficient included both wave drag and viscous drag components. However, the viscous drag component was relatively minor, typically contributing less than 7% to the total drag coefficient. Consequently, the results obtained by simulations in the turbulent regime were relatively similar to the inviscid case. As in the inviscid case for the NACA0012 airfoil examined earlier, all of the mean drag coefficients obtained by the stochastic simulations are smaller than the DSIM results for all of the optimized profiles considered. All of the airfoils show a high sensitivity to input parameter variation, with the most stable airfoil #791 only achieving minimum $CV(C_D)$ of 7.7% in the inviscid case and 7.9% in the turbulent regime. Once again, the hierarchy of stability is preserved.

The results of stochastic simulations of dense gas flow over the optimized airfoils pre-

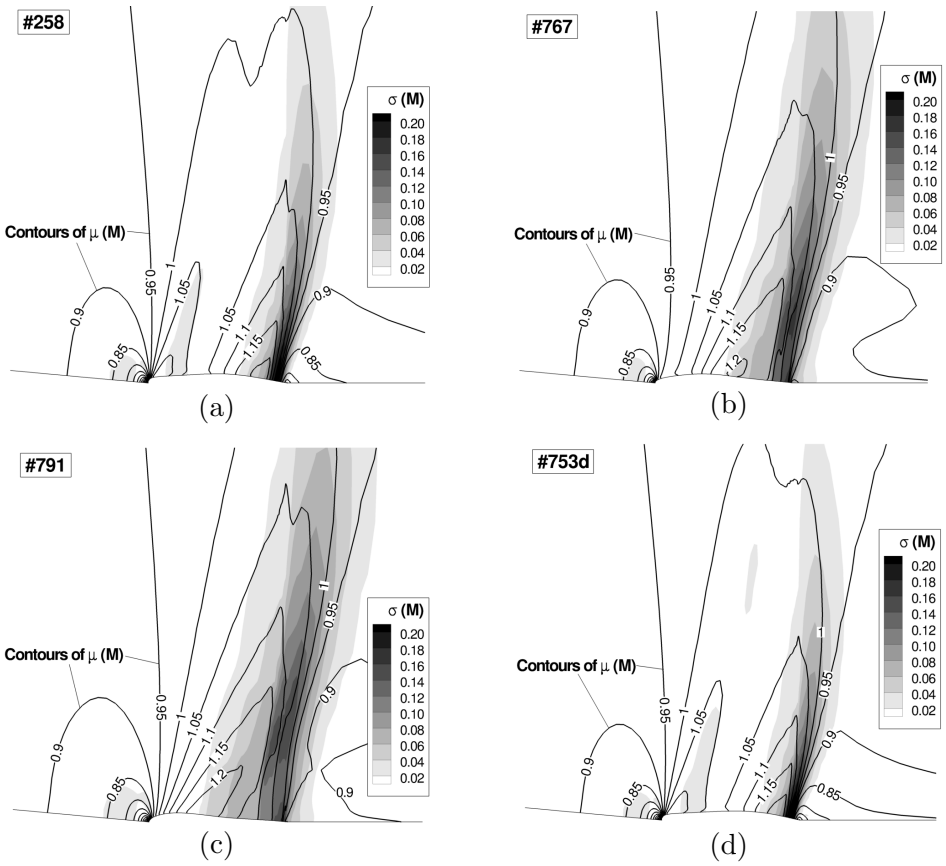

Figure 9: Contours of the mean μ and standard deviation σ of the Mach number for the optimized airfoils. ($N_p = 3$, medium grid 100×32). Airfoils (a) #258. (b) #767 (c) #791 and (d) #753d.

sented in Tables 3 and 4 show the trend that a highly stable airfoil can be obtained with a shallow trailing edge gradient. The price of this improved stability is an increased shock wave intensity and a subsequent increase in the drag coefficient. The characteristics of the turbulent dense gas flow over the most stable (#791), most unstable (#753d), and the NACA 0012 airfoils are presented in Figure 10, via contours of the mean and standard deviation of the Mach numbers. Superimposed on the contour plot of the mean Mach number values is a streamline representing the approximate extent of the separated recirculation bubble (when this is present). In the case of the unstable but low drag #753d airfoil, a small region of intense variation of the Mach number is observed at the base of the trailing edge shock. Additionally, the steep trailing edge gradient of this airfoil promotes the formation of a large region of separated flow. These two effects are largely responsible for the poor stability performance of this airfoil. On the other hand, the stabilizing effects of a shallow trailing edge gradient are clear for the #791 airfoil. The flow does not separate at the trailing edge, and the values of the standard deviation of the Mach number are lower than in the #753d airfoil case and are spread over a larger region

Airfoil Geometry	$C_D(DSIM)$	$\mu(C_D)$	$\sigma(C_D)$	$CV(C_D)$
NACA0012	0.0704	0.0669	0.0108	16.2%
#258	0.0544	0.0568	0.0099	17.5%
#767	0.0730	0.0707	0.0085	12.0%
#791	0.0821	0.0804	0.0064	7.9%
#753d	0.0467	0.0526	0.0104	19.9%

Table 4: Viscous drag coefficients (turbulent grid, 160×64 cells) for optimized airfoils, $N_p = 2$.

at the trailing edge. However, the cost of this increased stability is an increase in drag coefficient due to the formation of a stronger shock wave. The elevated cost of the two parameter stochastic optimization is justified when a compromise between a low mean drag coefficient and a small solution variation is desired. The airfoil #753d obtained from the single parameter optimization exhibits very high CV values of 24.5% (inviscid) and 19.9% (turbulent regime) for the same order of polynomial chaos, as the variation of the solution is not taken into account during the optimization procedure.

Note that for all of the simulations carried out in the present work, only the upper surface of the airfoils were considered. In this configuration, it is possible for a detached fluid flow to reattach to the virtual boundary downstream of the airfoil profile. In the full profile case, this is not possible and an unstable recirculation zone may be created. As a result, the airfoils with the lowest drag coefficients (#258, #753d) may eventually exhibit poorer drag performance in an unsteady simulation of the full profile. Overall, the robust optimization procedure based on a genetic algorithm coupled to a stochastic uncertainty quantification method proves to be a powerful design tool. The robust optimization provides detailed engineering information of system response to input parameter variation, which will allow increased design confidence. In the case of an ORC turbine where the input energy source is highly variable, predictable knowledge of the variation of system response is critical for evaluating system feasibility.

5 CONCLUSIONS

In the present work, a series of optimized airfoils was developed for dense gas flows under uncertain operating conditions using a robust optimization procedure based on a multi-objective genetic algorithm (MOGA). This type of analysis is essential in improving the feasibility of Organic Rankine Cycle (ORC) turbines, which are typically designed to recover energy from variable sources such as waste heat from industrial processes.

A validated[22] PCM algorithm with a subsequent RMC is then applied to an existing solver[23] of an inviscid transonic dense gas flow over half of a symmetrical NACA0012 airfoil at $M_\infty = 0.95$. The working fluid used is *pf-perhydrofluorene* ($C_{13}F_{22}$, commercially known as PP10) with the thermodynamic properties modeled by the Martin-Hou equation of state. The aerodynamic performance of the airfoil at 0° incidence is examined with Gaussian random variations in the upstream pressure and temperature. Using a small number of deterministic solutions, the PCM determined that the dense gas system was highly sensitive to input parameter variation, due to the large changes in physical flow behavior close the the inversion zone of PP10. In this zone where the fundamental

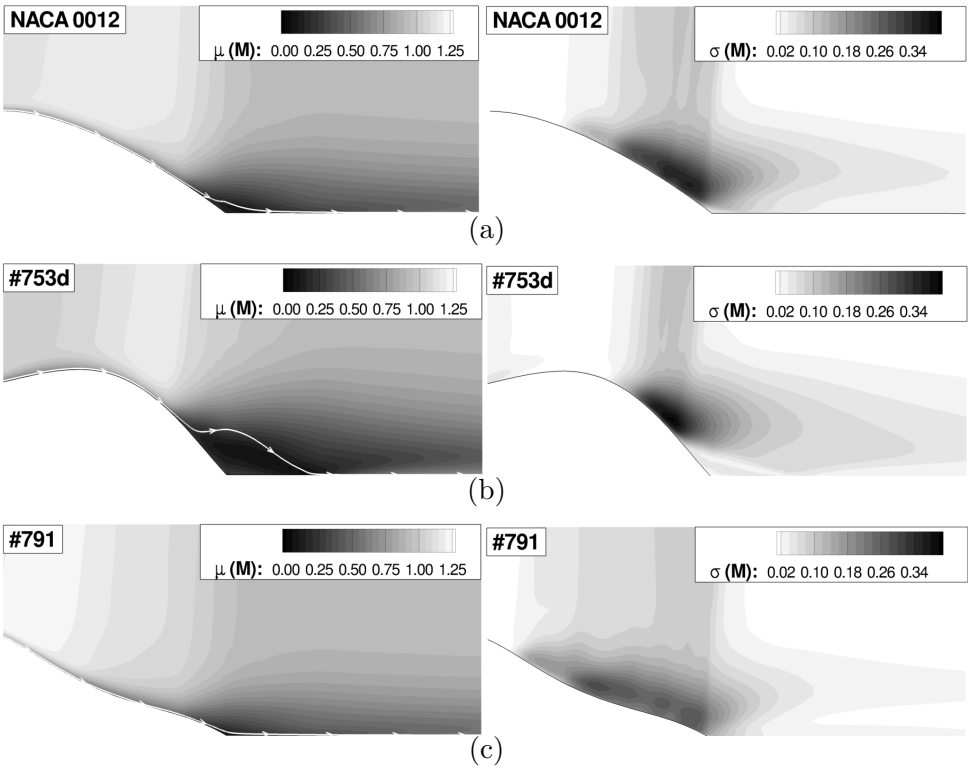

Figure 10: Contours of the mean (left) and standard deviation (right) of the Mach number for the airfoils (a) NACA 0012, (b) #753d [most unstable], (c) #791 [most stable]. The streamline shows the approximate extent of the separated flow. NB: aspect ratio not preserved.

derivative of gas dynamics $\Gamma > 0$, compression shock waves can be suppressed as a consequence of the entropy inequality. Furthermore, the set of statistical output solutions was found to be non-Gaussian, due to the non-linearity of the dense gas system, tending towards the low drag side.

Finally, the PCM analysis of the dense gas system with $N_p = 2$ was coupled with an existing MOGA based robust optimization procedure, which generated a series of optimized 2D airfoils for dense gas flows based on minimization of the mean and standard deviation of the drag coefficient. Several individual optimized geometries were selected from the final Pareto front which exhibited improvements in mean performance and/or stability over the NACA0012 airfoil. A posteriori testing of the the stochastic performance of these individuals was verified for a polynomial chaos order $N_p = 3$ on a standard medium grid (100×32 cells) grid in the inviscid case, and for $N_p = 2$ on a grid with a refined boundary layer (160×64 cells) in the turbulent regime simulation. The viscous drag component was found to be a relatively minor contributor to the overall drag coefficient, whereas the wave drag of the trailing edge shock proved to be the dominant factor. The position, intensity and sensitivity of the trailing edge shock to fluctuations in the operating conditions was modified by the geometry of the optimized individuals, which in

turn strongly influenced the drag coefficient. In particular, airfoils with a shallow trailing edge gradient were found to exhibit increased stability at the cost of an increased mean drag coefficient.

The two parameter stochastic robust optimization was compared to a standard deterministic optimization procedure where only the mean drag coefficient was optimized. The elevated cost of the two parameter stochastic optimization is justified when both a low mean drag coefficient and a small solution variation are desired. Several methods exist to mitigate the elevated computational cost of a multi-parameter optimization procedure. Large scale parallelization of the PCM analysis and the MOGA codes could be implemented with relative ease, as each collocation point of each individual in a generation could be calculated concurrently. Other methods to reduce calculation cost include surrogate models such as the Artificial Neural Network (ANN), already employed to shape optimization of dense gas flows.[25] Following the implementation of these computational cost reduction methods, multi-objective robust optimization procedures could help to develop the next generation of highly efficient turbomachinery. The present study has shown that a robust optimization based on a genetic algorithm coupled to a stochastic analysis proves to be a powerful design tool. The robust optimization provides detailed engineering information of system response to operating point variation, which could ultimately lead to refinements in the robust design of ORC turbines.

REFERENCES

[1] J. Horen, T. Talonpoika, J. Larjola and T. Siikonen. Numerical simulation of real-gas flow in a supersonic turbine nozzle ring. *J Eng Gas Turb Power*, **124**(2), 395–403 (2002).

[2] B. Brown and B. Argrow. Application of Bethe-Zel'dovich-Thompson fluids in organic rankine cycle engines. *J Propul Power*, **16**(6), 1118–1123 (2000).

[3] J. Monaco, M. Cramer and L. Watson. Supersonic flows of dense gases in cascade configurations. *J Fluid Mech*, **330**, 31–59 (1997).

[4] G. Angelino and C. Invernizzi. Supercritical heat pump cycles. *Int J Refrig*, **17**(8), 543–554 (1994).

[5] C. Zamfirescu and I. Dincer. Performance investigation of high-temperature heat pumps with various BZT working fluids. *Thermochim Acta*, **488**, 66–77 (2009).

[6] N. Kirillov. Analysis of modern natural gas liquefaction technologies. *Chem Petrol Eng*, **40**(7-8), 401–406 (2004).

[7] K. Lambrakis and P. Thompson. Existence of real fluids with a negative Fundamental Derivative Γ. *Phys Fluids*, **15**(5), 933–935 (1972).

[8] P. Thompson and K. Lambrakis. Negative shock waves. *J Fluid Mech*, **60**, 187–208 (1973).

[9] M. Cramer. Negative nonlinearity in selected fluorocarbons. *Phys Fluids*, **1**(11), 1894–1897 (1989).

[10] P. Colonna, N. Nannan, A. Guardone and T. van der Stelt. On the computation of the fundamental derivative of gas dynamics using equations of state. *Fluid Phase Equilibr*, **286**(1), 43–54 (2009).

[11] P. Thompson. A fundamental derivative in gas dynamics. *Phys Fluids*, **14**, 1843–1849 (1971).

[12] M. Cramer and A. Kluwick. On the propagation of waves exhibiting both positive and negative nonlinearity. *J Fluid Mech*, **142**, 9–37 (1984).

[13] M. Cramer and G. Tarkenton. Transonic flows of Bethe-Zel'dovich-Thompson Fluids. *J Fluid Mech*, **240**, 197–228 (1992).

[14] V. Maizza and A. Maizza. Unconventional working fluids in Organic Rankine-cycles for waste energy

recovery systems. *Appl Therm Eng*, **21**, 381–390 (2001).

[15] T. Hung, T. Shai and S. Wang. A review of Organic Rankine Cycles (ORCs) for the recovery of low-grade waste heat. *Energy*, **22**(7), 661–667 (1997).

[16] P. Cinnella and P. Congedo. Aerodynamic performance of transonic Bethe-Zel'dovich-Thompson flows past an airfoil. *AIAA Journal*, **43**, 370–378 (2005).

[17] P. Cinnella, P. Congedo and L. Pediroda. Quantification of thermodynamic uncertainties in real-gas flows. *Int J of Engineering Systems Modelling and Simulation*, **2**(1-2), 12–24 (2009).

[18] O. Knio and O. LeMaître. Uncertainty propagation in CFD using polynomial chaos decomposition. *Fluid Dyn Res*, **38**, 616–640 (2006).

[19] A. Loeven, J. Witteveen and H. Bijl. Efficient uncertainty quantification using a two-step approach with chaos collocation. In ECCOMAS CFD. TU Delft, Netherlands (2006).

[20] A. Loeven, J. Witteveen and H. Bijl. Probabilistic collocation: An efficient non-intrusive approach for arbitrarily distributed parametric uncertainties. In 45th AIAA Aerospace Sciences Meeting and Exhibit, AAIA Paper 2007-317. Reno, Nevada, USA (2007).

[21] R. Abgrall. A simple, flexible and generic deterministic approach to uncertainty quantification in non-linear problems: application to fluid flow problems. Tech. rep., INRIA (2008). `http://hal.inria.fr/inria-00325315/en/`.

[22] S. Hercus. Uncertainty quantification in the numerical simulation of complex aerodynamic flows. Master's thesis, Arts et Métiers ParisTech, Paris, France (2009).

[23] P. Cinnella and P. Congedo. Numerical solver for dense gas flows. *AIAA Journal*, **43**, 2458–2461 (2005).

[24] P. Congedo, C. Corre and P. Cinnella. Airfoil shape optimization for transonic flows of Bethe-Zel'dovich-Thompson fluids. *AIAA Journal*, **45**, 1303–1316 (2007).

[25] P. Cinnella and P. Congedo. Optimal airfoil shapes for viscous transonic flows of Bethe-Zel'dovich-Thompson fluids. *Comput Fluids*, **37**, 250–264 (2008).

[26] P. Cinnella and P. Congedo. GA-Hardness of aerodynamic optimization problems: Analysis and proposed cures. In 18th AIAA Computational Fluid Dynamics Conference, AAIA Paper 2007-3828. Miami, Florida, USA (2007).

[27] P. Cinnella and P. Congedo. Inviscid and viscous aerodynamics of dense gases. *J Fluid Mech*, **580**, 179–217 (2007).

[28] P. Cinnella. Transonic flows of dense gases over finite wings. *Phys Fluids*, **20**, 046103 (2008).

[29] P. Cinnella, P. Congedo and D. Laforgia. Transonic flows of BZT fluids through turbine cascades. In Proceedings of the 3rd ICCFD Conference, ISBN: 3-540-31800-3, 227–232. Springer-Verlag, Berlin, Toronto, Canada (2004).

[30] P. Congedo, P. Cinnella and C. Corre. Shape optimization for dense gas flows in turbine cascades. In Proceedings of ICCFD 4. Ghent, Belgium (2006).

[31] J. Martin and Y. Hou. Development of an equation of state for gases. *AIChE Journal*, **1**, 142–151 (1955).

[32] G. Emanuel. Assessment of the MartinHou equation for modeling a non-classical fluid. *J Fluids Eng*, **116**, 883–884 (1996).

[33] A. Guardone, L. Vigevano and B. Argrow. Assessment of thermodynamic models for dense gas dynamics. *Phys Fluids*, **16**, 3878–87 (2004).

[34] D. Xiu and G. Karniadakis. Modeling uncertainty in flow simulations via generalized polynomial chaos. **187**, 137–167 (2003).

[35] K. Deb. Multi-objective optimization using evolutionary algorithms. Wiley (2001).

[36] N. Srinivas and K. Deb. Multi-objective optimization using nondominated sorting genetic algorithms. *Evol Comput*, **2**, 221–248 (1994).